Numerical Analysis of Shock Wave Supported by Microwave Discharge in Microwave-Beaming Propulsion

IEPC-2015-467p／ISTS-2015-b-467p

Presented at Joint Conference of 30th International Symposium on Space Technology and Science 34th International Electric Propulsion Conference and 6th Nano-satellite Symposium, Kobe, Japan July 4–10, 2015

Yoshiaki Kageyama* and Masayuki Takahashi † and Naofumi Ohnishi‡
Tohoku University, Sendai, Miyagi, 980-8579, Japan

Two-dimensional simulations of microwave breakdown for extinction of remaining plasma at the first pulse were carried out by the finite difference time domain method coupled with an electron diffusion model for examing plasma formation in a microwave-beaming thruster. The plasma structure can be extinguished quickly without reducing thrust power by adding a small amount of SF6 to air. Three-dimensional simulations were also conducted for elucidation of the detailed plasma structure and the qualitative assessment of shock wave formation between two- and three-dimensional simulations in the view of heating rate and ionization front speed. The results suggested that two-dimensional simulations may underestimate the shock wave strength and then the thrust power because higher heating rate and lower ionization speed are obtained compared to three-dimensional simulations.

Nomenclature

D_a = ambient diffusion coefficient
D_e = electron diffusion coefficient
D_{eff} = effective diffusion coefficient
e = elementary charge
$\boldsymbol{E}$ = electric field
E_{eff} = local effective electric field
E_{rms} = local root-mean-square electric field
f = microwave frequency
$\boldsymbol{H}$ = magnetic field
$\boldsymbol{J}$ = current density
k = Boltzmann constant
L = characteristic diffusion length
m_e = electron mass
n_e = electron number density
p = ambient pressure
r_{ei} = recombination coefficient

*Mr, Department of Aerospace Engineering, kageyama@rhd.mech.tohoku.ac.jp
†Mr, Department of Aerospace Engineering, mtakahashi@rhd.mech.tohoku.ac.jp
‡Associate Professor, Department os Aerospace Engineering, ohnishi@rhd.mech.tohoku.ac.jp

t	=	time
T_e	=	electron temperature
$\boldsymbol{v}_e$	=	electron mean velocity
ϵ_0	=	permittivity of vaccum
λ	=	wavelength of incident microwave
λ_D	=	local Debye length
μ_0	=	permeability of vaccum
μ_e	=	electron mobility
μ_i	=	ion mobility
ν_a	=	attachment frequency
ν_i	=	ionization frequency
ν_m	=	electron-neutral momentum collision frequency
τ_M	=	local Maxwell relaxation time
ω	=	angular frequency

I. Introduction

Beamed energy propulsion (BEP) has been expected as a lower cost space transportation system than exsiting chemical propulsion.[1] Microwave-beaming propulsion which is one of the BEP schemes has two advantages compared to other BEPs because of its low development costs and high power ability.[2] In the microwave-beaming propulsion, a high-power microwave irradiates a flying veahicle from a ground base. Atmospheric discharge then occurs around a focal point of an on-board mirror and expands toward the microwave source followed by a shock wave. The thrust power must depend on the generated plasma structure and the ionization front propagation velocity because the shock wave is sustained by the microwave absorption by the plasma. However, it is difficult to investigate the relationship between the plasma formation and resultant thrust from the experiment. Numerical simulations may clear the relationship and give new knowledge to understand the plasma structure formation.

A number of experimental and numerical researches of the microwave breakdown have been conducted so far. In past experiment by Hidaka et al., the characteristic discharge structure were captured using a pulsed 1.5-MW, 110-GHz gyrotron for cases of different gas species and pressures.[3] In a air condition, in E-plane (a plane perpendicular to the magnetic field), the filamentary structures are formed with intervals of $\lambda/4$, stretching obliquely against the microwave source. On the other hand, in H-plane (a plane perpendicular to the electric field), the upstream filaments are regularly built by some discharge spot, and the downstream filaments are formed in a straight line with the same interval. Boeuf et al. carried out two-dimensional simulations of formations of filamentary plasma arrays.[4] The simulation result generally reproduced the characteristic structure observed in the experiments, but the width of plasma structure was estimated shorter than the experimental one in E-plane and the discharge structure were not formed in a straight line behind the ionization front. In three-dimensional simulations of the structure formation by Kourtzanidis et al., the propagation speed is smaller and obliquely extending speed is larger than the two-dimensional simulations. Also, the extension length is longer and the filamentary structure is unlimitedly extended after the initial breakdown.[5]

Furthermore the thrust impulse is decreased after the second pulse of multi-pulse in experiments about the thrust power of the microwave-beaming propulsion by Oda et al.[6] One of the reasons of this thrust lowering comes from the fact that focusing of the microwave is interrupted by the plasma produced by the first pulse.

In this paper, we conducted two-dimensional simulations of microwave breakdown for air and mixed gas for extinction of the remaining plasma at the first pulse and three-dimensional simulations of atmospheric discharge for a qualitative assessment of shock wave generation between two- and three-dimensional simulations from the view point of heating rate and ioinization front velocity.

II. Numerical Methods and Conditions

We solve Maxwell's equations for microwave propagation,

$$\nabla \times \mathbf{E} = \mu_0 \frac{\partial \mathbf{H}}{\partial t}, \tag{1}$$

$$\nabla \times \mathbf{H} = \epsilon_0 \frac{\partial \mathbf{E}}{\partial t} + \mathbf{J}. \tag{2}$$

The current density $\mathbf{J}$ is estimated by Ohm's law,

$$\mathbf{J} = -en_e \mathbf{v}_e. \tag{3}$$

The electron mean velocity $\mathbf{v}_e$ is given by solving the following equation of motion of electrons,

$$\frac{\partial \mathbf{v}_e}{\partial t} = -\frac{e\mathbf{E}}{m_e} - \nu_m \mathbf{v}_e, \tag{4}$$

where the electron-neutral momentum collision frequency $\nu_m = 5.3 \times 10^9 \cdot ps^{-1}$.[7]

To take into account diffusion of electrons, we couple the following electron diffusion equation with for above Maxwell's equations,

$$\frac{\partial n_e}{\partial t} - \nabla \cdot (D_{eff} \nabla n_e) = n_e (\nu_i - \nu_a) - r_{ei} {n_e}^2, \tag{5}$$

The diffusion flux of electrons is determined by the effective diffusion coefficient D_{eff} given by

$$D_{eff} = \frac{\alpha D_e + D_a}{\alpha + 1}, \tag{6}$$

$$\alpha = \nu_i \tau_M = {\lambda_D}^2 / L^2. \tag{7}$$

The transport coefficients are given by

$$D_e = \mu_e \frac{kT_e}{e}, \tag{8}$$

$$\mu_e = \frac{e}{m\nu_m}, \tag{9}$$

$$D_a = D_e/100, \tag{10}$$

$$\tau_M = \epsilon_0 / \left[en \left(\mu_i + \mu_a \right) \right], \tag{11}$$

$$L = \sqrt{D_e/\nu_i}. \tag{12}$$

Moreover, the local Debye length is estimated by $\lambda_D = \left(\epsilon_0 kT_e / e^2 n_e\right)^{\frac{1}{2}}$.[7]

Maxwell's equations (1) and (2) are numerically solved by Finite Difference Time Domain (FDTD) method coupling with the solution of the electron diffusion equation (5) using the second-order central difference method.

The simulation domain is depicted in Fig. 1 for two-dimensional simulations of extinguishing the remaining plasma. The grid size is $\lambda/200$, and the simulation domain covers $3\lambda \times 3\lambda$ in E-plane. The ambient pressure is 300 Torr. The incident uniform wave with 110 GHz and 6 MV/m is injected at $x = 0$ toward the x-direction. In this simulation, we suppose to the air mixed with another gas (sulfur hexafluoride, SF6). We use the classical assumption that the ionization and attachment frequencies ν_i and ν_a are functions (obtained from bolsig+[8]) of the local effective field E_{eff}:

$$E_{eff} = E_{rms} \left(1 + \frac{\omega^2}{{\nu_m}^2}\right)^{-\frac{1}{2}}. \tag{13}$$

The recombination coefficient r_{ei}=0. We used the first-order Mur boundary condition for Maxwell's equations and the first-order extrapolated open boundary for the electron diffusion equation.

In three-dimensional simulations, the simulation domain is shown in Fig. 2. For lower calculation costs, the grid size is $\lambda/50$ coarser than the two-dimensional simulations. In the three-dimensinal simulations about the atmospheric discharge, the ionization coefficient ν_i is estimated by a fitting formula constructed from past experimental data,[9,10]

$$\nu_i = \nu_a \left(\frac{E_{eff}}{E_c} \right)^{5.3}, \tag{14}$$

where ν_a=5.4 × 10^4 × p s^{-1}. the recombination coefficient is estimated by the empirical formula of $r_{ei} = 1.8 \times 10^{13} \times \left(\frac{300.0}{T_e[\mathrm{K}]}\right)^{0.39}$ $\mathrm{m^{-3}s^{-1}}$. The electron temperature T_e=2 eV.[?] The other conditions are the same as the two-dimensional simulations.

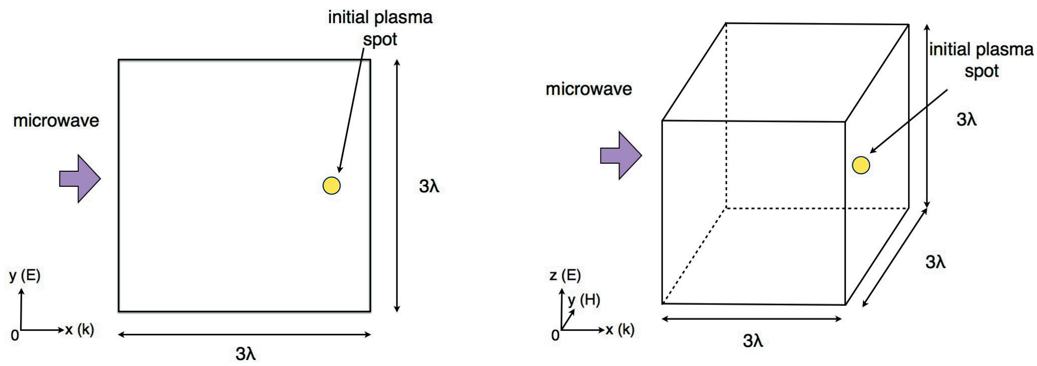

(a) two-dimensional simulation (b) three-dimensional simulation

Figure 1. Simulation domain

III. Results and Discussion

III.A. two-dimensional simulation of extinction of the remaining plasma

In this section, we conducted two-dimensional simulations of the plasma formation in air and mixed gas for extinguishing the remaining plasma. Figure 2 shows the electron number density at 13.6 ns in (a) the air and (b) mixed gas (air : SF6 = 9 : 1). The plasma in the air condition forms a characteristic filamentary structure that the plasma grows toward the microwave source, stretching obliquely. However, the filamentary structure are formed only around outer edge in the mixed gas. The electric field is decreased by the reflection at the ionization front in the right region. In the mixed gas, the attachment frequency is higher than the ionization frequency and the plasma is then extinguished in the weak electric field because SF6 acts as an insulator. So, the inner structure disappears in the mixed gas.

Fig. 3 shows the heating rate at 13.6 ns. The heating rates have similar distributions for the both cases and are high only around the outer edge of the plasma structure. Since the strength of a shock wave driven by the microwave depends on this heating rate, the expected thrust power must be the same for the both cases. Therefore, by adding a small amount of SF6 to the air, the remaining plasma can be extinguished quickly without reducing the resultant thrust power.

III.B. three-dimensional simulation of atmospheric discharge

In this section, we conducted three-dimensional simulations for examing the formation of the plasma structure. Figures 4, 5 and 6 show the isosurfaces of the electron number density of 1.3 × 10^{21} $\mathrm{m^{-3}}$ at (a) 131 and (b) 191 ns. Figures 4 and 5 are plotted when we take a line of sight parallel to the y- and z-axis, which correspond to E-plane and to H-plane, respectively. The filamentary structures are found with intervals of $\lambda/4$, stretching obliquely as shown in Fig. 4. This features agree with the experiments[3] and the previous numerical simulations.[4] The filaments on the left side are regularly built up by some discharge spots and on the right side are formed in a straight line with the same interval as shown in Fig. 5. This structure has

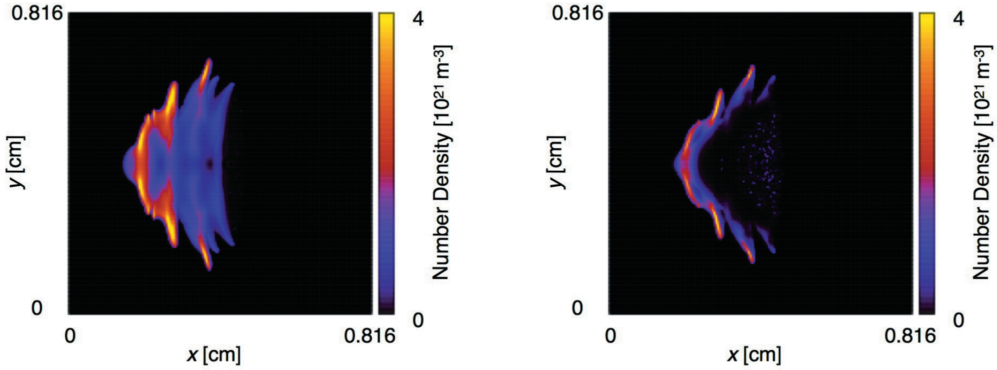

(a) air (b) mixed gas (air : SF6 = 9 : 1)

Figure 2. Contours of electron number density at 13.6 ns.

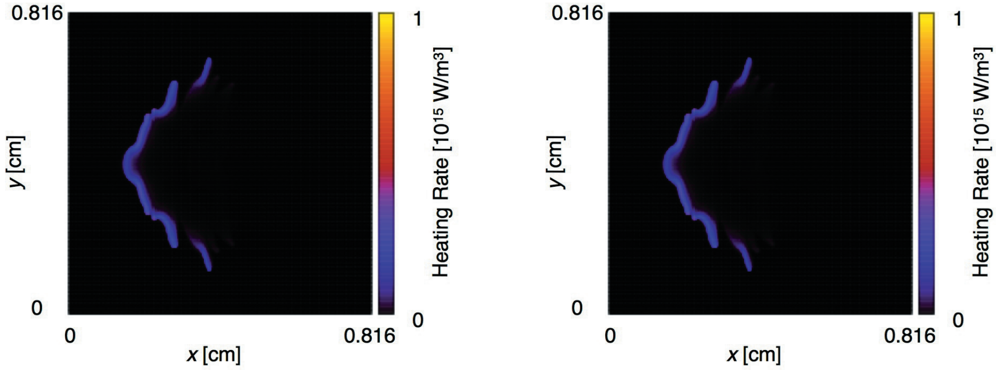

(a) air (b) mixed gas (air : SF6 = 9 : 1)

Figure 3. Contours of heating rate at 13.6 ns.

never been captured in two- and three-dimensional simulations, whereas it appears in the past experiments.[3] It is thought that past three-dimentional simulation domain and calculation time were too small to capture this structure.[5] Since the ionization fronts grow toward the microwave source in E-plane, the microwave begins not to be able to transmit this ionization fronts from the central axis. Therefore, the filamentary structures behind the ionization front begin to disappear from the central axis in Fig. 4. Moreover, this effect occurs not only the x-z plane at y=0 but also all the y-constant plane as shown in Fig. 6.

In this simulation, the width of the filamentary structure in E-plane has a finite size though the filamentary structure is unlimitedly elongated in the past three-dimensional simulation. The obtained extending length is 1.73 λ, whereas 0.78 λ in the two-dimensional simulation. At the initial process of the formation, the microwave can transmit backward by diffraction because the filamentary structure is thin in the y-direction as show in Fig. 6(a). So, the electric field intensity in the back side of the three-dimensional simulation is higher than the two-dimensional simulation, and the filamentary structure is elongated. When the filamentary structure is formed to some extent at 191 ns, the structure in H-plane has enough thickness preventing from diffraction. The microwave then could not transmit backward, resulting in stopping the extension and the shorter filamentary structure than one–third filaments (A in Fig. 6 (a)).

Figure 7 shows the heating rate obtained by two- and three-dimensional simulations along a line parallel to the z-direction centered at the extension axis (B axis in Fig. 6 (a)). The obtained discharge front propagation speed is listed in Table 1. The heating rates are about 3.5 $\times$ 10^{14} W/m^3 for the both cases, but one in the three-dimensional simulation is about twice larger than the two-dimensional results at the tip of filaments. The larger is the heating rate, the stronger a shock wave is generated. The resultant shock wave is therefore expected to be more stronger in the three-dimensional case. Furthermore, the propagation speed of the structure front in the 3D simulation is smaller than the 2D results as known in the past 3D simulations. Since the heating region can be confined in the thruster during a long time with the lower speeds, it is expected the thrust power is larger in the 3D simulations.

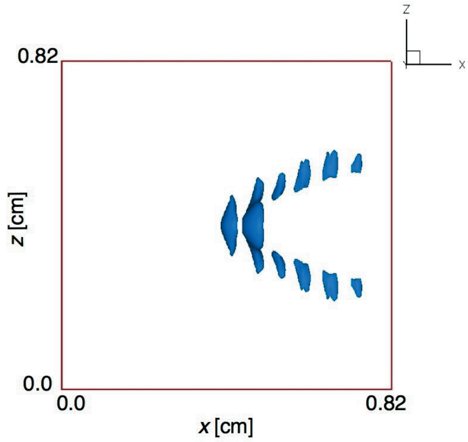

(a) t = 136 ns

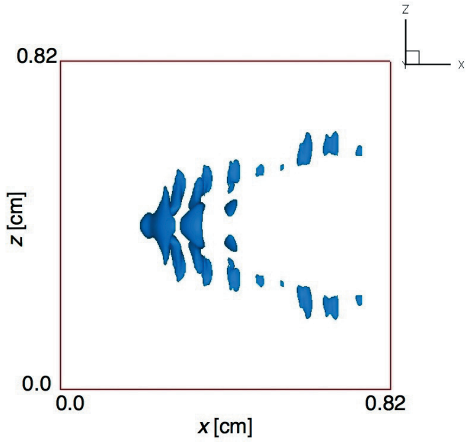

(b) t = 191 ns

Figure 4. Isosurfaces of electron number density of 1.3 × 10^{21} m^{-3} with a line-of-sight is parallel to the y-axis.

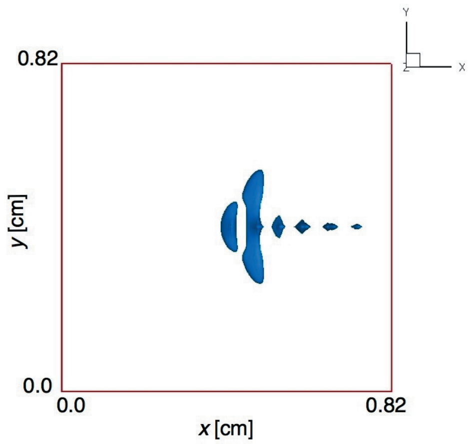

(a) t = 136 ns

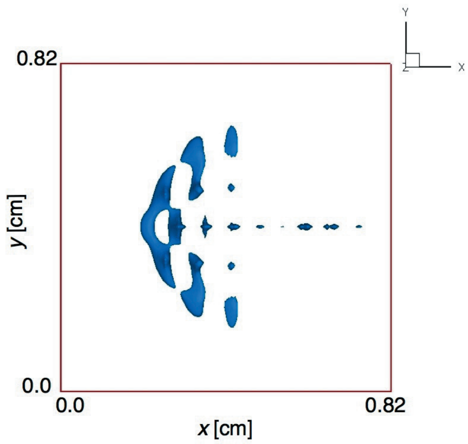

(b) t = 191 ns

Figure 5. Isosurfaces of electron number density of 1.3 × 10^{21} m^{-3} with a line-of-sight parallel to the z-axis.

IV. Conclusions

We have conducted two- and three-dimensional simulations of microwave air breakdown for examining plasma filaments formation and its effect on a shock generation.

From two-dimensional simulations of the plasma structure formation in air and mixed gases, it is found that the plasma structure can be extinguished quickly without reducing the thrust power by adding a small amount of SF6 to the air.

In the three-dimensional simulations, the upstream filaments are regularly built by some discharge spots, and the downstream filaments are formed in a straight line with the same interval. This feature well agrees with the experiments and has never been captured by the past numerical simulations. Moreover, the width

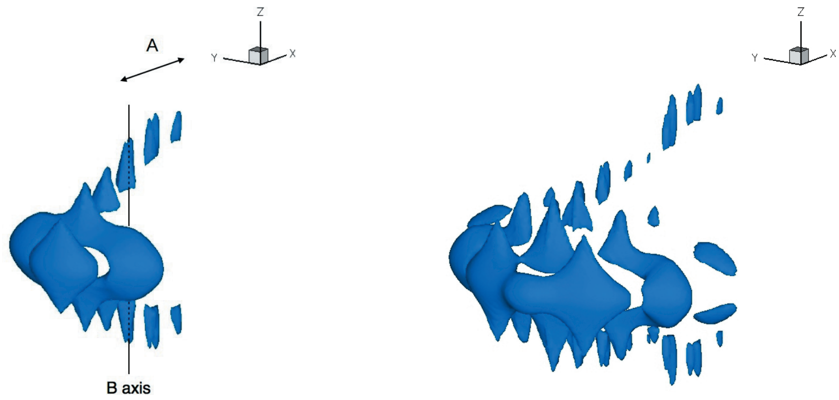

(a) $t = 131$ ns (b) $t = 191$ ns

Figure 6. Isosurfaces of electron number density of 1.3 $\times$ 10^{21} m^{-3} with another angle of view.

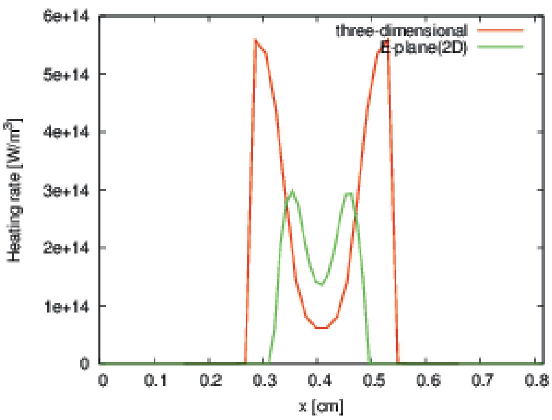

Figure 7. Heating rate obtained by two- and three-dimensional simulations along a line parallel to the z-direction centered at the extension axis (B axis).

of the filamentary structure in E-plane has a finite size though the structure is unlimitedly elongated in the past three-dimensional simulations. It is because the filamentary structure in H-plane has enough thickness prohibit the diffraction of the incident microwave after the structure grows to some extent. Thus, the microwave cannot much transmit backward by the diffraction, and the extension growth of the filamentary structure are suppressed.

The heating rate and the discharge front propagation speed are smaller in the three-dimensional case than the two-dimensional cases. It is expected that the generated shock waves and thrust power become larger in the actual discharge than the predicted ones by two-dimensional simulations.

References

[1]Katsurayama, H., Komurasaki, K., and Arakawa, Y., "Feasibility for the Orbital Launch by Pulse Laser Propulsion," Journal of Space Technology and Science, Vol. 20, 2004, pp. 32–42.

[2]Oda, Y., Komurasaki, K., Kasugai, A., and Sakamoto, K., "Plasma Generation Using High-Power Millimeter-Wave Beam and Its Application for Thrust Generation," Journal of Applied Physics, Vol. 100, 2006, 113307.

[3]Hidaka, Y., Choi, E. M., Mastovsky, I., Shapiro, M. A., Sirigiri, J. R., Temkin., R. J., Edmiston, G. F., Neuber, A. A., and Oda, Y., "Plasma Structures Observed in Gas Breakdown Using a 1.5 MW 110GHz Pulsed Gyrotron," Physics of Plasmas, Vol. 16, 2004, 055722.

Table 2. Discharge front propagation speed

	2D (E-plane)	2D (H-plane)	3D
propagation speed (km/s)	42	40	33

[4]Boeuf, J. P., Chaudhury, B., and Zhu, G. Q., "Theory and Modeling of Self-Organization and Propagation of Filamentary Plasma Array in Microwave Breakdown at Atmospheric Pressure," Physical Review Letters, Vol. 104, 2010, 015002.

[5]Kourtzanidis, K., Boeuf, J. P., and Rogier, F., "Three Dimensional Simulations of Pattern Formation during High-Pressure, Freely Localized Microwave Breakdown in Air," Phyics of Plasmas, Vol. 21, 2014, 123513.

[6]Oda, Y., "Experimental Study on Microwave Beaming Propulsion Using a High Power Gyrotron," Master's thesis, 2004.

[7]Chaudhury, B., Boeuf, J. P., and Zhu, G. Q., "Pattern Formation and Propagation during Microwave Breakdown," Physics of Plasmas, Vol. 17, 2010, 123505.

[8]Hagelaar, G. J. M., and Pitchford, L. C., "Solving the Boltzmann Equation to Obtain Electron Transport Coefficients and Rate Coefficients for Fluid Models," Plasma Sources Science and Technology, Vol. 14, 2005, pp. 722–733.

[9]Zhu, G. Q., Boeuf, J. P., and Chaudhury, B., "Ionization-diffusion plasma front propagation in a microwave field," Plasma Sources Science And Technology, Vol. 20, 2011, 035007.

[10]Warne, L. K., Jorgenson, R. E., and Nicolaysen, S. D., "Ionization coefficient approach to modeling breakdown in nonuiform geometries," SANDIA Report, Vol. SAND2003, 2003, 4078.